Arch Pharm Res Vol 25, No 6, 807-816, 2002

Archives of Pharmacal Research
http://apr.psk.or.kr

Flexible Docking of an Acetoxyethoxymethyl Derivative of Thiosemicarbazone into Three Different Species of Dihydrofolate Reductase

In-Hee Choi and Choonmi Kim

College of Pharmacy, Ewha Womans University, Seoul 120-750, Korea

(Received April 15, 2002)

Dihydrofolate reductases (DHFR) of human, *Candida albicans* and *E. coli* were docked with their original ligands of X-ray crystal complex using QXP (Quick eXPlore), a docking program. Conditions to reproduce the crystal structures within the root mean square deviation (rmsd) of 2.00 Å were established. Applying these conditions, binding modes and species-specificities of a novel antibacterial compound, N^4-(2-acetoxyethoxymethyl)-2-acetylpyridine thiosemicarbazone (AATSC), were studied. As the results, the docking program reproduced the crystal structures with average rmsd of six ligands as 0.91 Å ranging from 0.49 to 1.45 Å. The interactions including the numbers of hydrogen bonds and hydrophobic interactions were the same as the crystal structures and superposition of the crystal and docked structures almost coincided with each other. For AATSC, the results demonstrated that it could bind to either the substrate or coenzyme sites of DHFR in all three species with different degrees of affinity. It confirms the experimentally determined kinetic behavior of uncompetitive inhibition against either the inhibitor or the coenzyme. The docked AATSC overlapped well with the original ligands and major interactions were consistent with the ones in the crystal complexes. The information generated from this work should be useful for future development of antibacterial and antifungal agents.

Key words: Flexible docking, Thiosemicarbazone, DHFR, QXP program, Binding modes

INTRODUCTION

2-Acetoxyethoxymethyl (AEM) derivatives of thiosemicarbazone (TSC) have been synthesized and their antimicrobial activities were reported on *Staphylococcus aureus* (gram-positive), *E. coli* and *Pseudomonas aeruginosa* (gram-negative), *Candida albicans* (yeast), and *Aspergillus niger* (mold) (Foye *et al.*, 1986). Various mechanisms such as inhibition of dihydrofolate reductase (DHFR) or ribonucleotide reductase, metal chelation and DNA binding have been proposed to explain the activities. These compounds are composed of two open chains which are open chain analogues of ribosyl and triazine groups. The AEM moiety, already used in antiviral compounds, could be a possible conformational analogue of the ribosyl group of NADPH and the TSC moiety could mimic the triazine group which is found in a number of antifolate drugs. The most active of the derivatives, N^4-(2-acetoxyethoxymethyl)-2-acetylpyridine thiosemicarbazone (AATSC), was evaluated for its inhibition profile against bovine liver DHFR and reported to be a fully uncompetitive inhibitor of that enzyme with Ki of 2.9 ± 0.3 μM with respect to dihydrofolate (DHF), the substrate, and 3.3 ± 0.3 μM with respect to NADPH, the coenzyme (Lebrun *et al.*, 1990). The authors questioned the possibility of AATSC competing either with the ribosyl site of the nicotinamide mononucleotide ribose or that of the adenine mononucleotide ribose (or both) of the NADPH. They also questioned the possibility of hypothetical mimicry of a triazine group by the TSC moiety of AATSC. Their experiments suggested that AATSC should bind to the substrate site of the DHFR-NADPH binary complex. This assumption is consistent with the kinetic behavior of the uncompetitive inhibition. On the other hand, they proposed that the direct attachment to the free enzyme might be untenable due to the uncompetitive type of inhibition observed with AATSC. However, the structural similarity between the NADPH and AATSC suggests the

Correspondence to: Choonmi Kim, College of Pharmacy, Ewha Womans University, 11-1 Daehyun-dong, Seodaemoon-ku, Seoul 120-750, Korea
E-mail: cmkime@ewha.ac.kr

strong possibility that the compound may bind to the free enzyme in place of NADPH. Their kinetic study also revealed that, when AATSC was used together with MTX, some cooperative enhancement of MTX activity by AATSC was observed. This finding could be indicative of the location of the interaction site of AATSC inside DHFR. They suggested that the binding of AATSC might take place at a site different from that of the binding site for DHF and MTX (Foye *et al.*, 1998). The site could be an extra-site distant from the active site or the coenzyme site.

DHFR is a key enzyme in the synthesis of thymidylate and therefore of DNA. Inhibitors of the enzyme are used in treatment of several human diseases, namely, neoplastic diseases, bacterial, protozoal, fungal infections, and autoimmune diseases (Schweitzer *et al.*, 1990). As crystallographic information of DHFR is available from human and other species, it became possible to investigate the interactions of inhibitors with the binding sites of DHFRs by computer-aided molecular docking method. Computer docking programs have been developed to find out the most possible binding modes between ligands and proteins and to rank them based on the binding affinity. QXP, a program used in this study, adopts Monte Carlo perturbation with energy minimization in Cartesian space. It uses extensive conformational searching and energy minimization to identify the conformation a molecule is likely to adopt upon binding to enzyme. The program has powerful and rapid computer algorithms for docking and structure-based drug design (McMartin and Bohacek, 1997). There are several recent reports on the studies of molecular modelings using this program such as defining a common pharmacophore pattern in 3D space for fibrinogen receptor antagonist (Stilz *et al.*, 2001), docking diphosphonomethylphenylalanine into the phosphotyrosine pocket of the Src SH2/citrate crystal structure to determine whether the SH2 domain of Src could accommodate this novel amino acid (Bohacek *et al.*, 2001), structure-based designing to discover the nonpeptide inhibitors of Src (Shakespeare *et al.*, 2000; Metcalf III *et al.*, 2000), and docking of 1,2,4-oxadiazole analogues to the C- or N-terminal SH2 domain of tyrosine kinase ZAP-70 to find out potent and selective inhibitors (Vu *et al.*, 1999).

In this study we carried out computer aided molecular docking to locate the precise binding sites of AATSC in DHFR. Three different binding areas which are consisted of DHFR-NADPH binary complex, DHFR-ligand binary complex, and DHFR-free enzyme were targeted for AATSC binding. To establish species-specific binding modes of AATSC against DHFRs of different species, crystal structures of human, *Candida albicans* and *E. coli* were used for docking. The information obtained from this study may provide the action mechanism of the novel antibacterial agent, grounds for the selection of effective molecules out of many candidates and a rational basis for the design of novel inhibitors.

MATERIALS AND METHODS

Molecular modeling was performed on Silicon Graphics Octane/SE Workstation running QXP docking module of the FLO96 molecular modeling program (McMartin and Bohacek, 1997).

Preparation of enzymes for docking

The crystal structures of DHFRs were selected from the Protein Data Bank that satisfy the conditions of having no mutations and forming ternary complex with the coenzyme and an inhibitor. For human enzyme, 1HFR (huDHFR) with 187 residues, complexed with $NADP^+$ and furo[2,3D] furopyrimidine (MOT) was selected. For yeast and bacterial enzymes, 1AOE of *Candida albicans* (caDHFR), with 192 residues, complexed with NADPH and 7-(1-ethylpropyl)7H-pyrrolo-[3.2-F]quinazoline-1,3-diamine (GW345), and 1RX2 of *E. coli* (ecDHFR), with 159 residues, complexed with $NADP^+$ and folate (FOL) were chosen, respectively. The sequence identity of caDHFR is 27% to the huDHFR and 30% to the ecDHFR. They all have the same general folds of an extended central β-sheets with flanking α-helices (Whitlow *et al.*, 1997). All the crystallographic water atoms were removed except those known to participate in the reaction. Polar hydrogen atoms were added to both the enzyme and the ligand. The entire complex was then energy minimized for docking.

Preparation of ligands for docking

The original ligands in the crystal structures, MOT, GW345, FOL, and NADP(H) were used to test the reproducibility. As a novel antibacterial agent, AATSC was used. These molecules are presented in Table I with their structures. AATSC was first built on the screen using QXP, hydrogens were removed from carbons and then minimized. With this structure, conformational search was carried out to generate a set of low energy conformations. The best conformation with often the lowest energy and good orientation was chosen for the docking study.

Flexible docking simulation

Docking process can be divided into two phases. One is the searching algorithm, which finds possible binding geometries of the protein and its ligand. The other is the scoring function, which ranks the searching results and selects out the best binding geometry. In this study docking was carried out by using the MCDOCK conformational searching/energy minimization procedure of QXP. It uses Monte Carlo simulation as a searching algorithm and modified version of the Amber force field for scoring function (Weiner

Table I. Names and structures of ligands used for docking study

Enzyme	Ligand Code	Chemical Name	Structure
huDHFR	MOT	N-[4-(2,4-Diaminofuro(2,3D)pyrimidine-5-yl)methylamino]-benzoyl-1-glutamate	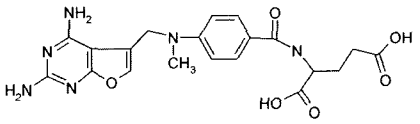
caDHFR	GW345	1,3-Diamine-7-(1-ethyl-propyl)-7H-pyrrolo-[3,2-F]quinazoline	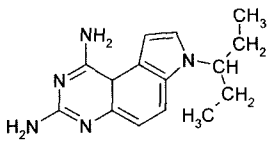
ecDHFR	FOL	4-(2-Amino-4-oxopteridin-6-yl) methylaminobenzoyl-L-glutamicacid	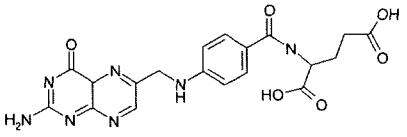
NADPH	NADPH	Nicotinamide Adenine Dinucleotide Phosphate	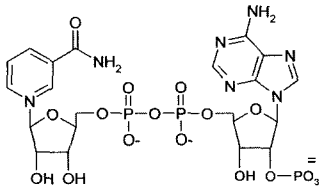
AATSC	AATSC	N^4-(2-Acetoxyethoxymethyl)-2-acetylpyridine thiosemicarbazone	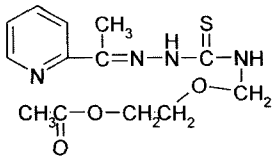

et al., 1984).

The binding site model includes all residues within 8-10 Å of the ligand. During conformational searching and energy minimization, only residues of the enzyme that are known to change conformation upon binding with different ligands are allowed to move freely, whereas ligands are set fully flexible. Six water molecules are left in the active site of huDHFR, one in caDHFR and four in ecDHFR (Meiering *et al.*, 1995a; 1995b; Bystroff *et al.*, 1990). To prepare the first docking set, the original ligands in the crystal structures were extracted from the ternary complexes. Docking was performed on the resulting binary complexes of DHFR-NADP(H). The second set was DHFR-ligand binary complex from which the coenzyme was extracted. For the third set, both the ligand and the coenzyme were removed and docking was carried out on the resulting DHFR-free.

For docking searches, the binding site cavity must be defined. In order to do so, several atoms of flexible residues lining the active site, one atom from each residue, are marked with light blue. This forms a gray mesh area where a ligand enters. These atoms are called marker atoms and they should point into the cavity and be a few angstroms from the edge of the cavity. A ligand was located immediate outside of the active site for simulation to make sure it enters the cavity even though prelocating the ligand inside with proper orientation makes docking much faster and easier. Each ligand was subjected to 5000 cycles of conformational searching and energy minimization. Each cycle involved 400 rapid Monte Carlo search steps followed by energy minimization of the best conformation from the set of 400. The program returns the 25 lowest energy conformations for visual inspection (Shakespeare *et al.*, 2000).

Evaluation methods

Docking results were evaluated first using the criteria of energy and scoring values such as the total interaction energy (Eass), internal ligand energy (Elig), contact energy (Ecnt), hydrogen bonding score (Nhbd), and hydrophobic contact score (Nhph). Eass is evaluated as good if it is below -30 kJ/mole and Elig should be less than 10 kJ/mole (Metcalf III *et al.*, 2000). The second criterion was the rmsd of the best docked position with respect to the position of the crystal structure. This is a generally accepted value to evaluate the quality of docking results. A ligand position with rmsd less than 2.00 Å is usually considered as a well docked solution (ligand rmsd). When the two

ligands are different, the rmsd was calculated by comparing the conformation of flexible residues in the enzyme of docked complex with respect to the same residues in the crystal structure (residue rmsd). The third and probably the most important criterion was the visual inspection on the screen of the interactions between the enzyme and inhibitors in the docked complex. Surface which represents hydrogen bond acceptor (red), hydrogen bond donor (blue) and hydrophobic atoms (yellow) of the active site was used to study the interactions (Vu *et al.*, 1999). WebLab Viewer was also used.

RESULTS

Reproducibility

Three original inhibitors and three coenzymes were extracted one at a time from the ternary complexes and then docked back into the resulting binary complexes of each target enzyme from three different species. RMSD was calculated for each docked conformation and presented in Table II with total energies. McMartin, the program developer, reported the average rmsd of ten original ligands as 0.76 Å for his reproducibility test (McMartin and Bohacek, 1997). In our study the docking reproduced the crystal structures with rmsd of 0.49 Å, 0.72 Å and 1.45 Å for inhibitors and 0.89 Å, 0.84 Å and 1.06 Å for coenzymes in *C. albicans*, human and *E. coli* DHFRs, respectively. The average rmsd of the above six ligands was 0.91 Å, demonstrating an excellent reproducibility of the program. Eass obtained which are in between -74.1 and -330 kJ/mol imply the stability of the complexes formed by docking. Fig. 1 shows docked complex structures superimposed on the original crystal structures. As the docked inhibitors and coenzymes nearly coincided with the original ones in the crystal structures, the interactions were almost the same.

Docking of AATSC into huDHFR, caDHFR, and ecDHFR

Table III presents the docking data for the complexes formed between AATSC and each docking set of DHFRs from three different species. The average residue rmsd of nine sets was 0.64 Å and Eass was in the range of -68.8

Table II. Ligand rmsd and total energy values for reproducibility test

Enzyme	Ligand	RMSD (Å)	Total Energy (kJ/mol)
huDHFR	MOT	0.72	-170
	$NADP^+$	0.84	-330
caDHFR	GW345	0.49	-74.1
	NADPH	0.89	-290
ecDHFR	FOL	1.45	-166
	$NADP^+$	1.06	-312

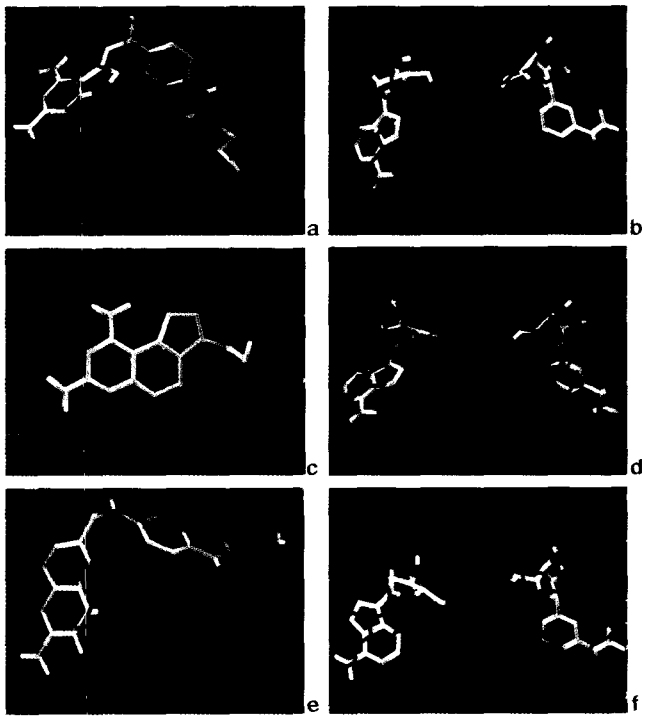

Fig. 1. Superimposition of docked and crystal structures for reproducibility. Ligands: MOT (a) and $NADP^+$ (b) for human DHFR, GW345 (c) and NADPH (d) for *C. albicans* DHFR, and FOL (e) and $NADP^+$ (f) for *E. coli* DHFR. atom color: ligands after docking, red: ligands in crystal structure.

Table III. Docking data for AATSC with each docking set of DHFRs from three different species

Enzyme	Docking set	RMSD (Å)	Eass[a] (kJ/mol)	Elig[b] (kJ/mol)	Eest[c] (kJ/mol)	Ecnt[d] (kJ/mol)	Nhbd[e]	Nhph[f]
huDHFR	DHFR-$NADP^+$	0.63	-84.8	1.4	-7.3	-49.4	1	5
	DHFR-MOT	0.61	-91.7	1.7	-10.8	-56.1	2	3
	DHFR-Free	0.67	-108	2.8	-8.3	-43.4	2	3
caDHFR	DHFR-$NADP^+$	0.50	-68.8	7.3	-3.5	-54.9	2	5
	DHFR-MOT	0.67	-108	8.2	-14.2	-59.2	3	4
	DHFR-Free	0.60	-113	9.0	-23.9	-51.6	5	3
ecDHFR	DHFR-$NADP^+$	0.59	-68.8	1.8	-8.5	-45.0	1	3
	DHFR-MOT	0.79	-108	1.2	-3.8	-49.8	2	4
	DHFR-Free	0.66	-106	6.6	-21.3	-54.9	5	5

[a]the total energy, [b]the internal strain energy of the ligand, [c]electrostatic energy, [d]contact energy, [e]the hydrogen bond score, [f]the hydrophobic contact score

to -113 kJ/mole. All other energy outputs were reasonable for the best docked conformations presented here. Binding modes are given below.

huDHFR. For the huDHFR-NADP$^+$ binary complex, AATSC was docked into the substrate site with one H-bond (Fig. 2a). The acetylpyridine (AP) moiety superimposed on the 2,4-diamino-furopyrimidine moiety of MOT (Fig. 2b). The pyridine ring formed van der Waals (vdw) contacts with the side chain of Glu-30 and the carbonyl of Ile-7, and a strong hydrophobic interaction with the side chain of Phe-34. The acetyl group made vdw contacts with the carbonyl of Val-115 and the hydroxyl of Tyr-121. These interactions are similar with the ones in the crystal structure, however, since the AP moiety has fewer nitrogen than the 2,4-diamino-furopyrimidine, the pyridine nitrogen atom does not H-bond with the carbonyls of conserved residues Val-115 and Ile-7 and with the hydroxyl of a conserved residue Tyr-121 (Cody *et al.*, 1998; Cocco *et al.*, 1983). Among the six long-lived bound water molecules, Wat-138 made a hydrophilic contact with the AP moiety. This suggests that the pyridine ring binds to the enzyme active site by undergoing electrophilic aromatic substitution reactions (Bruice, 1995) due to water, like a well known inhibitor, MTX, does at pKa 5.7 (Graffner-Nordberg *et al.*, 2000). The thiosemicarbazone (TSC) moiety superimposed well on N-methyl of the para-aminobenzoic acid (PABA) moiety of MOT. It occupied a hydrophobic environment surrounded by the side chain of Leu-22 and the main chain of Phe-31. The sulfur of the moiety contacted with the main chain of Ser-59 and the nitrogen of the moiety with the side chain of Leu-22 (Cody *et al.*, 1998). The 2-acetoxyethoxymethyl (AEM) moiety superimposed on parts of both the PABA and glutamate moieties of MOT. There was a hydrophobic contact between the side chain of Phe-31 and the moiety, which was generally shown in classical inhibitors of DHFR (Cody *et al.*, 1993). The acetoxy oxygen atom of this moiety formed one H-bond with the side chain of Asn-64.

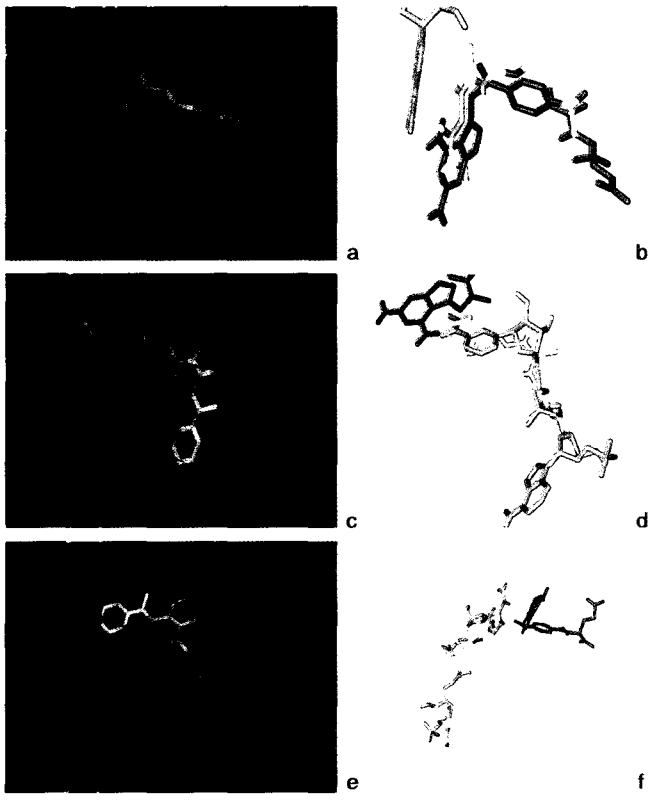

Fig. 2. Docking of AATSC into huDHFR-NADP$^+$ binary complex (a), huDHFR-MOT binary complex (c) and huDHFR-free (e), and superimposition with the original ligands in crystal structures(b,d,f, respectively). The mesh is an accessful surface of the binding site which is useful for showing steric and chemical complementarity. atom color: AATSC, red: MOT, orange: NADP$^+$.

For the huDHFR-MOT binary complex, AATSC was docked into the coenzyme site with two H-bonds in an extended conformation just like the NADP$^+$ of the crystal structure (Fig. 2c). The AP moiety superimposed on the nicotinamide ring of the NADP$^+$ (Fig. 2d). The pyridine ring formed a vdw contact with the main chain of the conserved residue Ala-9 (Cody *et al.*, 1997) and the ring carbon made nonbonded C-H···O contacts with neighboring oxygens of residue Ile-16 and Val-115 (Bolin *et al.*, 1982; Cody *et al.*, 1992). The TSC moiety overlapped with the nicotinamide-ribose group. It formed one H-bond with the main chain of Ser-119 and a vdw contact with the side chain of Ile-16. The AEM moiety overlapped with both nicotinamide and adenine phosphates. The oxygen of the moiety formed one H-bond with the main chain of Gly-20. It formed vdw contacts with Gly-117 and the side chain of Lys-55 but it did not interact with Lys-54 which is involved in potential electrostatic interactions to the negatively charged phosphate group in crystal structure (Cody *et al.*, 1997), probably because AATSC is shorter than NADPH in length.

For the huDHFR-free, AATSC formed two H-bonds with the residues of the coenzyme site but had no interaction with substrate site (Fig. 2e). The TSC moiety H-bonded to the side chain of Glu-116 and the AEM moiety to the main chain of Arg-79 (Fig. 2f). However, it did not completely dock itself even into the coenzyme site. Only part of the TSC and the AEM moieties overlapped with the nicotinamide phosphate and the nicotinamide ring, respectively. The AP moiety and two nitrogens of the TSC moiety bent away from the coenzyme site, resulting in poor interactions with the enzyme.

caDHFR. For the caDHFR-NADPH binary complex, AATSC was docked into the substrate site forming two H-bonds (Fig. 3a). Both the AP and the TSC moieties overlapped with the pyrroloquinazoline ring of GW345 (Fig. 3b). The pyridine ring formed a vdw contact with the car-

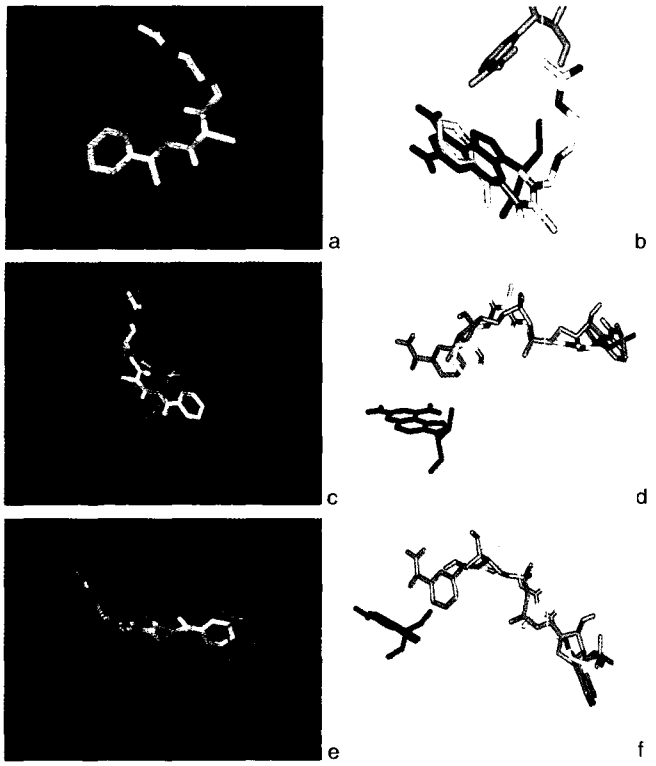

Fig. 3. Docking of AATSC into caDHFR-NADPH binary complex (a), caDHFR-GW345 binary complex (c) and caDHFR-free (e), and superimposition with the original ligands in crystal structures (b, d, f, respectively). The mesh is an accessful surface of the binding site which is useful for showing steric and chemical complementarity. atom color: AATSC, red: GW3, orange: NADPH.

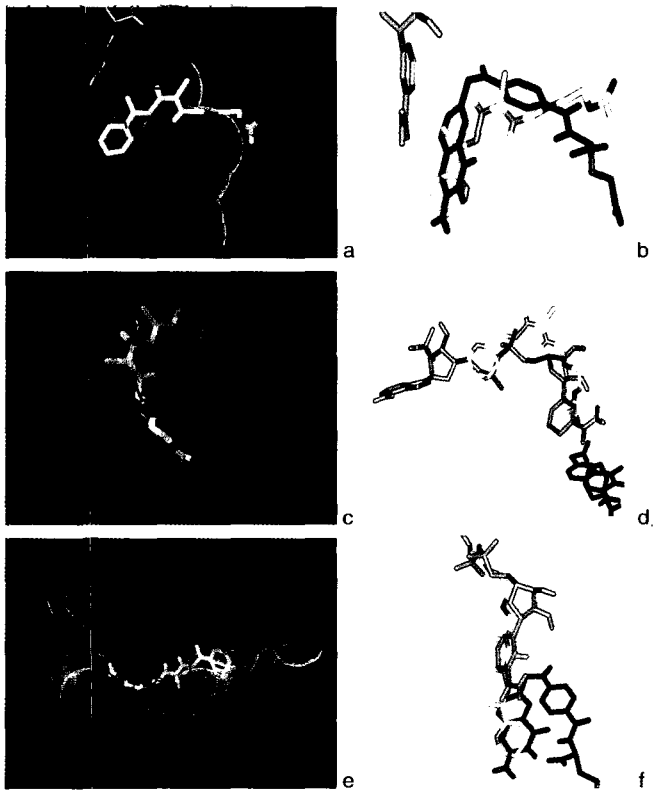

Fig. 4. Docking of AATSC into ecDHFR-NADP$^+$ binary complex (a), ecDHFR-FOL binary complex (c) and ecDHFR-free (e), and superimposition with the original ligands in crystal structures (b, d, f, respectively). The mesh is an accessful surface of the binding site which is useful for showing steric and chemical complementarity. atom color: AATSC, red: FOL, orange: NADP$^+$.

boxylate group of Glu-32, and vdw and hydrophilic contacts with the backbone carbonyl groups of Ile-9 and Ile-112, respectively. Similar interactions are shown in the crystal structure where Glu-32 and Ile-9 are involved in hydrogen bonding formation (Whitlow *et al.*, 1997). Part of the AEM moiety overlapped with the 3-pentyl substituent of GW345. The moiety orients perpendicular to the TSC moiety and positions in a hydrophobic region having interaction near the side chain of Ile-62. The moiety formed two H-bonds with the nicotinamide ring and the main chain of Gly-23.

For the caDHFR-GW345 binary complex, AATSC was docked into the coenzyme site with three H-bonds formed (Fig. 3c). The AP moiety overlapped with the nicotinamide ribose group (Fig. 3d). The moiety H-bonded with the side chain of Thr-58. The TSC moiety overlapped with the nicotinamide phosphate group. The AEM moiety overlapped with the adenine ribose group. The moiety formed two H-bonds to the side chains of Lys-57 and Gly-114. Since AATSC is shorter than NADPH, it did not bind to either the nicotinamide moiety or the adenine portion of NADPH. Therefore interactions with the residues such as Ala-11 or Glu-120 were not found (Whitlow *et al.*, 1997).

For the caDHFR-free, AATSC was docked into the coenzyme site forming five H-bonds (Fig. 3e). The AP moiety overlapped with the nicotinamide ribosyl group (Fig. 3f). The moiety formed a H-bond with the main chain of Ala-115. The TSC moiety overlapped with both the nicotinamide and the adenine phosphate groups. The moiety formed two H-bonds with its two nitrogens and the side chain of Glu-116. The AEM moiety overlapped with the adenine ribosyl group. It formed two H-bonds with Ser-78 and Arg-79. The compound did not reach to the nicotinamide moiety but was docked into the wide area of the coenzyme site probably because caDHFR is less flexible.

ecDHFR. For the ecDHFR-NADP$^+$ binary complex, AATSC was docked into a deep hydrophobic cleft where the FOL binds in crystal structure forming one H-bond (Fig. 4a). The AP moiety overlapped with the 2-amino-4-oxopteridine ring of FOL (Fig. 4b). This moiety formed a hydrophilic contact with the side chain of Asp-27. We assume that this residue causes protonation at nitrogen of the pyridine ring since residue Asp-27's role is to catalyze substrate protonation at the pteridine N5 by relaying a proton. It also formed vdw contacts with the backbone at conserved Ile-5 and the nicotinamide of NADP$^+$ as shown

in crystal structure (Bystroff *et al.*, 1990). An important residue, Phe-31 is situated above the acetyl of the AP moiety making a hydrophobic contact with the ligand. The TSC moiety overlapped with the PABA moiety of FOL. It formed vdw contacts with the backbone of conserved Ile-94 and the side chain of Met-20 which in the crystal structure showed the same interaction with the pteridine of FOL. The AEM moiety overlapped with part of the glutamate of FOL. The AEM moiety which is flexible like glutamate of FOL formed one H-bond with the side chain of Arg-52 (Bystroff *et al.*, 1990).

For the ecDHFR-FOL binary complex, AATSC was docked in an extended conformation into the coenzyme site with two H-bonds (Fig. 4c). The AP moiety overlapped with both adenine and nicotinamide phosphates of $NADP^+$ (Fig. 4d). The nitrogen of pyridine ring that overlaps with the adenine phosphate group formed one H-bond with His-45. The pyridine ring of AP made a hydrophobic contact with the side chain of Val-99 and a vdw contact with the main chain of Gly-96. However, AATSC showed no interaction with not only Gln-102 but also all residues in the adenine site because it is shorter than the $NADP^+H$ in length so it overlapped with the adenine phosphate group, not with the adenine moiety. The TSC moiety overlapped with nicotinamide phosphate of $NADP^+$. Sulfur of this moiety formed the second H-bond with the side chain nitrogen of Asn-18. It also formed a hydrophilic contact with Thr-46 (Sawaya and Kraut, 1997). The AEM moiety overlapped with both nicotinamide ribose and nicotinamide ring. It formed vdw contacts with the carboxyl oxygen of Ile-14 and the backbone of Ala-19. There is a hydrophilic contact between the sulfur of Met-20 and the oxygens of this moiety. The acetyl group of the moiety formed a vdw contact with Oγ1 of Thr-46 and the moiety has a hydrophilic contact with the main chain of Ile-94.

For the ecDHFR-free, AATSC was docked into both the substrate and the coenzyme sites forming five H-bonds (Fig. 4e). The AP moiety overlapped with the pteridine ring of FOL and the rest of AATSC overlapped with the coenzyme (Fig. 4f). The AP moiety formed a vdw contact with the side chain of Met-20. The TSC moiety overlapped with the nicotinamide ring of the coenzyme. The nitrogens of the moiety formed two H-bonds with Wat-324 and the main chain of Ile-94. The AEM moiety overlapped with the nicotinamide ribose and the two phosphate groups. It formed three H-bonds with the side chains of His-45, Thr-46 and Wat-423.

Species-specificity demonstrated by docking

Fig. 5 shows the species differences in binding modes of three different docking sets. In the DHFR-NADP(H) binary complexes (a), ligands were docked into the substrate sites with same orientations in all three species. However, the ligand in caDHFR occupied wide space probably because the active site cleft is significantly wider than those of the other two species (Whitlow *et al.*, 1997). HuDHFR is known to have rigid active site cleft due to closed conformation where the loop seals the active site (Sawaya and Kraut, 1997). Thus the AEM moiety which is the flexible part of AATSC was extended to be accommodated within the rigid cleft. In the DHFR-substrate binary complexes (b), ligands were all docked into the coenzyme site but the ones in huDHFR and caDHFR were docked with same orientations while the other in ecDHFR with opposite direction. It has been known that the structure of caDHFR is in general more similar to huDHFR and their sequence identity in the active site is significantly higher than ecDHFR (Gokhale *et al.*, 2000). This may be the reason why the orientations are similar in these two species (Whitlow *et al.*, 1997). In the DHFR-free (c), the ligand in huDHFR was not accommodated fully in the coenzyme site, while the one in caDHFR was docked well into the site. On the

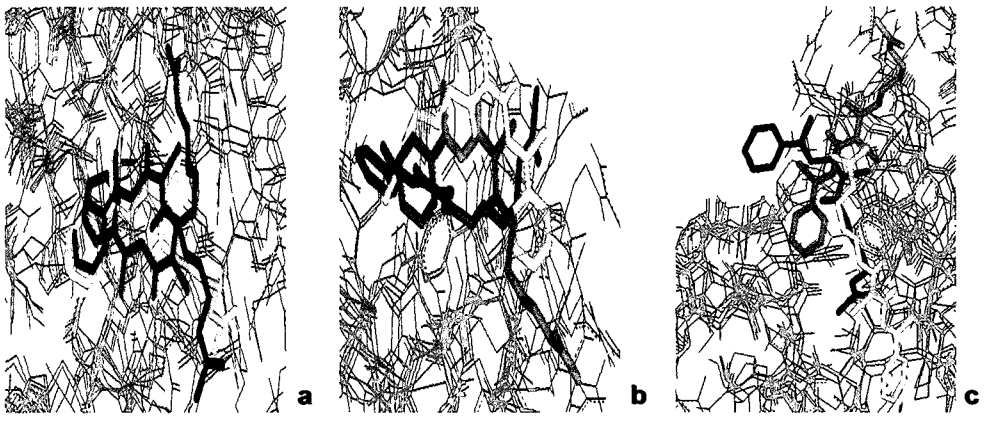

Fig. 5. Superimposed structures of AATSC docked into huDHFR, caDHFR and ecDHFR. AATSC was docked into DHFR-NADP (H) binary complex (a), DHFR substrate binary complex (b) and DHFR-free (c) from three different species. red: AATSC in caDHFR, blue: AATSC in huDHFR, yellow: AATSC in ecDHFR.

other hand, the ligand in ecDHFR occupied parts of both substrate and coenzyme sites. The coenzyme sites of DHFRs are polar in all three species (Gokhale *et al.*, 2000). Therefore, the polar AEM moiety was docked into that polar area in these enzymes. However, the AP moiety was located in different positions in all three species. Especially in ecDHFR the moiety reached deeply into the substrate site probably because the substrate site of ecDHFR is more flexible.

DISCUSSION

Proteins are dynamic molecules. They undergo conformational fluctuation under native conditions. Therefore flexible docking gives more accurate results compared to rigid docking even though it takes longer for much complicated calculations. The target enzyme in this study, DHFR, has two ligands, NADPH and DHF. Binding to either the coenzyme or substrate sites affects the affinity of DHFR for the other ligand (Fierke *et al.*, 1987). Jacques *et al.* reported that NADPH binds the free enzyme first prior to substrate in homoserine dehydrogenase reaction (Jacques *et al.*, 2001). Under physiological conditions where NADPH is in excess, this ligand is assumed to bind first in other dehydrogenase reactions too. Binding of NADPH to the free enzyme changes the conformation of the protein to accommodate the substrate the best way. Therefore inhibitors are supposed to bind to the DHFR-NADPH binary complex. AATSC, the ligand in this study, indeed binds well to the DHFR-NADP(H) binary complex in all three species confirming the experimental data of uncompetitive inhibition for the enzyme (Lebrun *et al.*, 1990). At constant DHF concentration, AATSC was also reported as showing an uncompetitive behavior against the coenzyme. It implies that at excessive concentration, DHF binds to DHFR prior to NADPH forming DHFR-DHF binary complex and AATSC binds to the coenzyme site, showing uncompetitive kinetics of inhibition. To see if it really happens, docking was carried out on DHFR-substrate binary complex. Our results demonstrated in all three species that it can bind to the coenzyme site as well overlapping with NADPH. There has been no known coenzyme inhibitor of DHFR yet, so AATSC could become a first good candidate for it. Especially when the ligand was docked into the DHFR-free enzyme, it interacted with residues in the coenzyme site with significant differences in the position and affinity of binding between species. The best docking was accomplished in caDHFR with five H-bonds (Fig. 6) and good position and orientation, presenting the strong possibility for developing novel antifungal coenzyme inhibitors. The results were fare with ecDHFR but not as good with huDHFR. The enhancing effect of MTX by AATSC may also be explained by the potential that binding to the coenzyme site of free enzyme changes conformation thereby increasing the affinity of MTX to the substrate site.

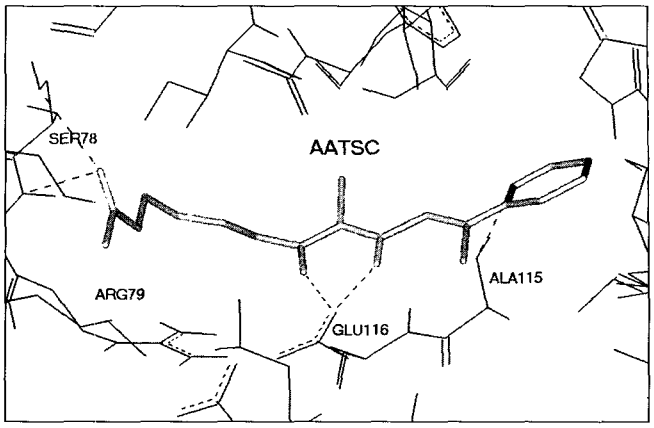

Fig. 6. Binding orientation of AATSC with caDHFR coenzyme site residues with hydrogen bonds depicted.

The AEM moiety which was postulated to be an open chain analogue of ribose, was bound in place of adenine ribose in caDHFR and nicotinamide ribose in ecDHFR. On the other hand, the TSC moiety was overlapped with pyrroloquinazoline ring of GW345, a triazine analogue, only in caDHFR but no other species. The results suggest that AATSC is a molecule better suited as a ribose analogue, again giving the possibility of becoming a coenzyme inhibitor. These findings provide the requisite foundation for future exploitation of DHFR in species-specific inhibitor design.

ACKNOWLEDGMENTS

This work was supported by the Intramural Research Grant of Ewha Womans University (2000) and the grant from the Research Institute of Pharmaceutical Sciences of Ewha Womans University (1999).

REFERENCES

Bohacek, R. S., Dalgarno, D. C., Hatada, M., Jacobsen, V. A., Lynch, B. A., Macek, K. J., Merry, T., Metcalf III, C. A., Narula, S. S., Sawyer, T. K., Shakespeare, W. C., Violette, S. M., and Weigele, M., X-ray structure of citrate bound to Src SH2 leads to a high-affinity, bone-targeted Src SH2 inhibitor. *J. Med. Chem.*, 44, 660-663 (2001).

Bolin, J. T., Filman, D. J., Matthews, D. A., Hamlin, R.C., and Kraut, J., Crystal structures of *Escherichia coli* and *Lactobacillus casei* dihydrofolate reductase refined at 1.7 resolution. *J. Biol. Chem.*, 257(22), 13650-13662 (1982).

Bruice, P. Y., *Organic Chemistry* (fourth eds). Prentice Hall, New Jersey, (1995).

Bystroff, C., Oatley, S. J., and Kraut, J., Crystal structures of *Escherichia coli* dihydrofolate reductase: the $NADP^+$ holoen-

zyme and the folate $NADP^+$ ternary complex: Substrate binding and a model for the transition state. *Biochemistry*, 29, 3263-3277 (1990).

Cody, V., Luft, J. R., Ciszak, E., Kalman, T. I., and Freisham, J. H., Crystal structure determination at 2.3 of recombinant human dihydrofolate reductase ternary complex with NADPH and methotrexate--tetrazole. *Anticancer Drug Design*, 7, 483-491 (1992).

Cody, V. Wojtczak, A., Kalman, T. I., Freisham, J. H., and Bladley, R. L., Conformational analysis of human dihydrofolate reductase inhibitor complexes: Crystal structure determination of wild type and F31 mutant binary and ternary inhibitor complexes. Ayling, J. E., Nair, M. G. and Baugh, C. M. (Eds.), In *Chemistry and Biology of Pteridines and Folates*. Plenum Press, New York, pp. 48-486, (1993).

Cody, V., Galitsky, N., Luft, J. R., Pangborn, W., Gangjee, A., Devraj, R., Queener, S. F., and Blakley, R. L., Comparison of ternary complexes of *Pneumocystis carinii* and wild type human dihydrofolate reductase with coenzyme NADPH and a novel classical antitumor furo[2,3-d]pyrimidine antifolate. *Acta Crystallographica*, D53, 638 (1997).

Cody, V., Galitsky, N., Luft, J. R., Pangborn, W., Blakley, R. L., and Gangjee, A., Comparison of ternary crystal complexes of F31 variants of human dihydrofolate reductase with NADPH and a classical antitumor furopyrimidine. *Anticancer Drug Des.*, 13, 307-315 (1998).

Cocco, L., Roth, B., Temple, C. Jr., Montgomery, J. A., London, R. E., and Blakley, R. L., Protonated state of methotrexate, trimethoprim, and pyrimethamine bound to dihydrofolate reductase. *Arch. Biochem. Biophys.*, 226, 567-577 (1983).

Fierke, C. A., Johnson, K. A., and Benkovic, S. J., Construction and evaluation of the kinetics scheme associated with dihydrofolate reductase from *Escherichia coli*. *Biochemistry*, 26 4085-4092 (1987).

Foye W. O., Banijamali, A. R. and Patarapanich, C., Synthesis and antimicrobial activities of N^4-(2-acetoxyethoxymethyl) thiosemicarbazones and N^3-(2-acetoxyethoxymethyl) thioureas. *J. Pharm. Sci.*, 75, 1180-1184 (1986).

Foye W. O., Dabade, S. V., Kelly, C. J., Lebrun, E., and van Rapenbusch, R., Synthesis and dihydrofolate reductase inhibitory activity of N4-2-L-glutaryl-N1-heteroaryl thiosemicarbazones. *Med. Chem. Res.*, 8, 542-553 (1998).

Gokhale, V. M., and Kulkarni, V. M., Selectivity analysis of 5-(arylthio)-2,4-diaminoquinazolines as inhibitors of Candida albicans dihydrofolate reductase by molecular dynamics simulations. *J. Comput. Aided Mol., Des.* 14, 495-500 (2000).

Graffner-Nordberg, M., Marelius, J., Ohlsson, S., Persson, A., Sverdberg, G., Anderson, P., Andersson, S. E., Aqvist, J., and Hallberg, A., Computational predictions of binding affinities to dihydrofolate reductase: Synthesis and biological evaluation of methotrexate analogues. *J. Med. Chem.*, 43, 3852-3861 (2000).

Jacques, S. L., Ejim, L. J., and Wright, G. D., Homoserine dehydrogenase from Saccharomyces cerevisiae: Kinetic mechanism and stereochemistry of hydride transfer. *Biochim. Biophys. Acta*, 1544, 42-54 (2001).

Lebrun, E., Tu, Y. X., van Rapenbusch, R., Banijamali, A. R., and Foye, W. O., Inhibition of bovine dihydrofolate reductase and enhancement of methotrexate sensitivity by N^4-(2-acetoxyethoxymethyl)-2-acetylpyridine thiosemicarbazone. *Biochim. Biophys. Acta.*, 1034, 81-85 (1990).

McMartin, C., and Bohacek, R. S., QXP: Powerful, rapid computer algorithms for structure-based drug design. *J. Comput. Aided Mol. Des.*, 11, 333-344 (1997).

Meiering, E. M., and Wagner, G., Detection of long-lived bound water molecules in complexes of human dihydrofolate reductase with methotrexate and NADPH. *J. Mol. Biol.*, 247, 294-308 (1995a).

Meiering, E. M., Li, H., Delcamp, T. J., Freisheim, J. H., and Wagner, G., Contributions of tryptophan 24 and glutamate 30 to binding long-lived water molecules in the ternary complex of human dihydrofolate reductase with methotrexate and NADPH studied by site-directed mutagenesis and nuclear magnetic resonance spectroscopy. *J. Mol. Biol.*, 247, 309-325 (1995b).

Metcalf III, C. A., Eyermann, C. J., Bohacek, R. S., Haraldson, C. A., Varkhedkar, V. M., Lynch, B. A., Bartlett, C., Violette, S. M., and Sawyer, T. K., Structure-based design and solid-phase parallel synthesis of phosphorylated nonpeptides to explore hydrophobic binding at the src SH2 (Src SH2) domain. *J. Comb. Chem.*, 2, 305-313 (2000).

Sawaya, M., and Kraut, J., Loop and subdomain movements in the mechanism of escherichia coli dihydrofolate reductase: Crystallographic evidence. *Biochemistry*, 36, 586-603 (1997).

Schweitzer, B. I., Dicker, A. P., and Bertino, J. R., Dihydrofolate reductase as a therapeutic target. *FASEB J.*, 4, 2441-2452 (1990).

Shakespeare, W., Yang, M., Bohacek, R., Cerasoli, F., Stebbins, K., Sundaramoorthi, R., Azimioara, M., Vu, C., Pradeepan, S., Metcalf III, C., Haraldson, C., Merry, T., Dalgarno, D., Narula, S., Hatada, M., Lu, X., van Schravendijk, M. R., Adams, S., Violette, S., Smith, J., Guan, W., Bartlett, C., Herson, J., Luliucci, J., Weigele, M., and Sawyer, T., Structure-based design of an osteoclast-selective, nonpeptide Src homology 2 inhibitor with in vivo antiresorptive activity. *Proc. Natl. Acad. Sci.*, 97, 9373-9378 (2000).

Stilz, H. U., Guba, W., Jablonka, B., Just, M., Klingler, O., Konig, W., Wehner, V., and Zoller, G., Discovery of an orally active non-peptide fibrinogen receptor antagonist based on the hydantoin scaffold. *J. Med. Chem.*, 44, 1158-1176 (2001).

Vu, C. B., Corpuz, E. G., Merry, T. J., Pradeepan, S. G., Bartlett, C., Bohacek, R. S., Botfield, M. C., Eyermann, C. J., Lynch, B. A., MacNeil, I. A., Ram, M. K., van Schravendijk, M. R., Violette, S., and Sawyer, T. K., Discovery of potent and selective SH2 inhibitors of the tyrosine kinase ZAP-70. *J. Med. Chem.*, 42, 4088-4098 (1999).

Weiner, S. J., Kollman, P. A., Case, D. A., Singh, U. C., Ghio, C., Algona, C., Profeta, S., and Weiner, P., A new force field for molecular mechanical simulation of nucleic acids and proteins. *J. Am. Chem. Soc.*, 106, 765-784 (1984).

Whitlow, M., Howard, A. J., Stewart, D., Hardman, K. D., Kuyper, L. F., Baccanari, D. P., Fling, M. E., and Tansik, R. L., X-ray crystallographic studies of *Candida albicans* dihydrofolate reductase: High resolution structures of the holoenzyme and an inhibited ternary complex. *J. Biol. Chem.*, 48, 30289-30298 (1997).